ELSEVIER

www.elsevier.nl/locate/jorganchem

Journal of Organometallic Chemistry 604 (2000) 34–42

Journal of Organometallic Chemistry

The organometallic double metal cyanide $[(Me_2Sn)_3\{Co(CN)_6\}_2\cdot 6H_2O]$. A three-dimensional framework of infinite, stapled ribbons

Eric Siebel [a], R. Dieter Fischer [a,*1], Nicola A. Davies [b], David C. Apperley [b], Robin K. Harris [b,*2]

[a] *Institut für Anorganische und Angewandte Chemie der Universität Hamburg, Martin-Luther-King-Platz 6, 20146 Hamburg, Germany*
[b] *Department of Chemistry, University of Durham, South Road, Durham DH1 3LE, UK*

Received 24 November 1999; accepted 7 March 2000

Abstract

The admixture of aqueous Me_2SnCl_2–Me_3SnCl solutions to solutions of $K_3[Co(CN)_6]$ in the molar ratios 3:0:2 and 1:1:1, respectively, affords precipitates of $[(Me_2Sn)_3\{Co(CN)_6\}_2\cdot 6H_2O]$ (**1**) and $[(Me_2Sn)(Me_3Sn)Co(CN)_6]$ (**2**). Another synthesis of **2** is based upon the bromination of $[(Me_3Sn)_3Co(CN)_6]$ in MeOH. The crystal structure analysis of **1** reveals stacks of infinite planar ribbons built up of *trans*-$Me_2Sn(\mu\text{-}NC)_4$ and *trans*-$Me_2Sn(\mu\text{-}NC)_2(OH_2)_2$ units as well as of *trans*-$Co(CN)_2$ fragments with terminal CN-ligands. $Sn\leftarrow OH_2\cdots(NC)_2$ hydrogen bonds interlink adjacent ribbons. Multinuclear (^{13}C, ^{15}N, ^{59}Co, ^{119}Sn) CPMAS solid-state NMR studies of **1** suggest some intra-ribbon dynamics, and help in proposing both a plausible architecture for anhydrous **2** and a better understanding of the nature of another precipitate **5** resulting from the admixture of a Me_2SnCl_2/Me_3SnCl solution to a solution of $K_4[Fe(CN)_6]$ (1:2:1).

Keywords: Double metal cyanide; Three-dimensional framework; Stapled ribbons

1. Introduction

For more than 25 years, double metal cyanide complexes, reminiscent in their composition of Prussian blue, have been known to catalyze the polymerization of epoxides to high molecular weight polyether polyols [1]. In particular, zinc hexacyanocobaltate(III), $[Zn_3\{Co(CN)_6\}_2]$, in the presence of $ZnCl_2$, diglyme and water, leads to polymers with narrow molecular weight distributions and exceptionally low levels of unsaturation [2]. According to the current patent literature, the search for continuously more efficient, double metal cyanide catalysts is ongoing [3]. As two new *organometallic* Prussian blue derivatives, and likewise potential epoxide polymerization catalysts, we describe here the supramolecular assemblies $[(Me_2Sn^{IV})_3\{Co^{III}(CN)_6\}_2\cdot 6H_2O]$ (**1**) and $[(Me_2Sn^{IV})(Me_3Sn^{IV})Co^{III}(CN)_6]$ (**2**). While the $\{Me_3Sn\}^+$ ion usually adds *two* more NC-ligands to achieve trigonal bipyramidal (tbp) configuration, the $\{Me_2Sn\}^{2+}$ ion is known to prefer coordinative saturation in affording a pseudo-octahedral $\{Me_2Sn(NC)_4\}$ unit [4]. In analogy to the well-known *super*-Prussian blue derivative $[(Me_3Sn)_3Co(CN)_6]$ (**3**), wherein each of the six cyanide nitrogen atoms occupies one axial coordination site of a Me_3Sn fragment [5], four cyanide N atoms of usually different $Co(CN)_6$ units are required to satisfy the four still available sites of each Me_2Sn fragment. As an instructive oxygen-bridged example, the coordination polymer $[Me_2SnMoO_4]$ is known to span a 3D framework of $SnMe_2O_4$ quasi-octahedra and MoO_4 tetrahedra [6]. In the following, we present the crystal structure of **1** and demonstrate spectroscopically that **2** is actually a novel 'alloyed' polymer (Me_2Sn:Me_3Sn), and not a mixture of **1** and **3**. Moreover, another precipitate potentially formulated as the likewise 'alloyed' new coordination polymer: $[(Me_2Sn)(Me_3Sn)_2Fe(CN)_6\cdot 3H_2O]$ (**5**) will be described

[1] *Corresponding author. Tel.: +49-40-4283831001; fax: +49-40-428382882.
[2] *Corresponding author.

0022-328X/00/$ - see front matter
PII: S0022-328X(00)00198-4

and critically inspected by solid-state magnetic resonance spectroscopy.

2. Preparation of 1, 2 and 5

Immediately on addition of an aqueous solution of Me_2SnCl_2 to an aqueous solution of $K_3[Co(CN)_6]$ in the molar ratio 3:2, a voluminous white precipitate is formed (Eq. (1)):

$$3Me_2SnCl_2 + 2K_3[Co(CN)_6] \rightarrow [(Me_2Sn)_3\{Co(CN)_6\}_2 \cdot x H_2O]\downarrow \quad (1)$$

The elemental analysis of the white powder obtained after filtration, washing (H_2O, Et_2O) and drying is more consistent with the presence of two H_2O molecules per formula unit ($x = 2$) than with $x = 6$, as actually indicated by the crystallographic results (vide infra). From the initially clear filtrate, transparent, plate-like single crystals suitable for crystallographic studies were deposited after a few days. Interestingly, the reaction of Me_2SnCl_2 and $K_3[Co(CN)_6]$ in the stoichiometric ratio 3:1 (instead of 3:2, see Eq. (1)) does not afford the potential 3D-polymer $[(Me_2SnCl)_3Co(CN)_6]$ (**4**), wherein each tin atom would suitably be 'functionalized' for various substitution reactions.

Analytically pure, and practically anhydrous, $[(Me_2Sn)(Me_3Sn)Co(CN)_6]$ (**2**) was obtained, in strict analogy to the preparation of **1** (Eq. (1)) from aqueous solutions of Me_2SnCl_2, Me_3SnCl and $K_3[Co(CN)_6]$ (1:1:1). During alternative attempts to prepare the brominated homologue of **4** following the well established bromination route of R_3SnR' systems [7]:

$$[(Me_3Sn)_3Co(CN)_6] + 3Br_2 \rightarrow [(Me_2SnBr)_3Co(CN)_6]\downarrow + 3MeBr \quad (2)$$

we also arrived exclusively at **2** and unreacted Br_2. Actually, **2** is obtained stoichiometrically in methanolic solution according to Eq. (3):

$$[(Me_3Sn)_3Co(CN)_6] + Br_2 \xrightarrow{(MeOH)} [(Me_2Sn)(Me_3Sn)Co(CN)_6] + Me_3SnBr + MeBr \quad (3)$$

The potential quasi-homologue $[(Me_2Sn(Me_3Sn)_2Fe(CN)_6 \cdot 3H_2O]$ (**5**) of **2** was prepared from Me_2SnCl_2, Me_3SnCl and $K_4[Fe(CN)_6]$ (1:2:1) by co-precipitation in H_2O. Spectroscopic results (vide infra) indicate that here the formation of $[(Me_3Sn)_4Fe(CN)_6]$ [8] is not strictly circumvented. In principle, the latter polymer and a new species to be formulated as $[Me_2Sn)_2Fe(CN)_6 \cdot x H_2O]$ could be expected instead of **5**. Interestingly, in the absence of Me_3SnCl (2:1 Me_2SnCl_2–$K_4[Fe(CN)_6]$), only a gel-like precipitate losing about 30% of its initial weight on drying was obtained, the filtration of which turned out to be extremely difficult. A similar 'cyanogel' is reported to result from $SnCl_4$ and $K_4[Fe(CN)_6]$ [9].

Table 1
Crystal data and structure refinement parameters of **1**

Empirical formula	$C_9H_{12}N_6O_3CoSn_{1.5}$
Formula weight (g mol^{-1})	489.12
Temperature (K)	153(2)
Crystal system	Orthorhombic
Space group	*Pbmn* (No. 62)
a (pm)	1038.0(0)
b (pm)	2419.2(9)
c (pm)	1485.6(4)
V (10^6 pm^3)	3731(2)
Z	8
D_{calc} (g cm^{-3})	1.742
Diffractometer/wavelength	Hilger & Watts Y290, Mo–K_α
Absorption coefficient (cm^{-1})	28.95
F(000)	1872
Θ-Range (°)	$2.39 < \Theta < 25.06$
Index range (°)	$-1 \le h \le 12$, $-1 \le k \le 28$, $-1 \le l \le 17$
Reflections collected	4349
Independent reflections	3451
Absorption correction (DIFABS)	T_{min}/T_{max}: 0.324/0.754
Data/restraints/parameters	3351/48/213
R indices (all data) R_1/wR_2	0.0909/0.2119
Final *R* indices ($I > 2\sigma$) R_1/wR_2	0.0572/0.1487
Largest diff. peak and hole (e $\times 10^{-6}$ pm^{-3})	1.765 and −1.418

3. Crystal structure of 1

The low-temperature single-crystal structure analysis of **1** confirms the presence of four well-positioned, and two strongly disordered, interstitial water molecules per formula unit. Crystal data and structure refinement parameters are given in Table 1, and the basic structure of this coordination polymer is shown in Fig. 1. As expected, all tin atoms are quasi-octahedrally coordinated, carrying their two methyl groups throughout in *trans*-orientation. While there are three different $\{Me_2Sn\}$ building blocks in the asymmetric unit, just one $\{Co(CN)_6\}$ entity is present. Only one of the three tin atoms adopts the initially expected $Me_2Sn(NC)_4$ pattern, while the composition of the other two $\{Me_2SnX_4\}$ units is $\{SnMe_2(NC)_2(OH_2)_2\}$. As four of the six water molecules are coordinated to tin atoms, two (*trans*-oriented) cyanide ligands of each Co atom must remain terminal. The basic structure elements of **1** are about 1.5 nm broad (i.e. from Sn1 to Sn2 via Sn3) and ca. 0.6 nm thick (i.e. from N3 to N5) ribbons of infinite length. While the surfaces of these ribbons are expected to be more hydrophobic owing to the specific orientation of the methyl groups, their edges should be

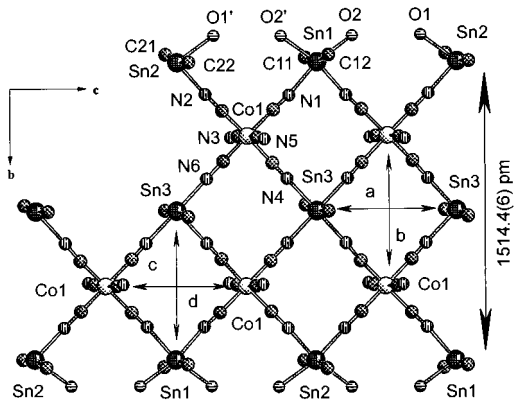

Fig. 1. View on the fragment of one $[(Me_2Sn)\{Me_2Sn(H_2O)_2\}_2\{Co(CN)_6\}_2]$ ribbon of **1** (extending along *c*), including the atomic numbering scheme. Hydrogen atoms have been omitted. a = Sn3···Sn3′: 763.3(3) pm, b = Co1···Co1′: 742.8(3) pm; c = Sn1···Sn3: 757.0(3) pm, d = Co1···Co1′: 745.0(3) pm.

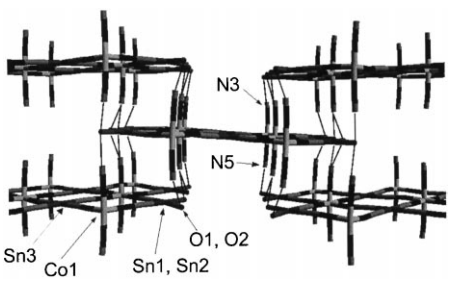

Fig. 2. Supramolecular architecture of **1**: view along *c*, depicting in the *a*/*b* plane the traces of five equivalent ribbons. Inter-ribbon O–H···NC hydrogen bonds (see the text) are indicated by faint straight lines. Methyl groups (bonded to Sn atoms) have been omitted.

Table 2
Selected interatomic distances (pm) and bond angles (°) of **1** [a]

Sn1–N1	226.3(9)	C1–N1–Sn1	172.8(8)
Sn2–N2	221.6(9)	C2–N2–Sn2	175.8(8)
Sn3–N4	230.1(10)	C4–N4–Sn3	175.8(10)
Sn3–N6	225.5(13)	C6–N6–Sn3	175.1(10)
Sn1–O2	231.4(8)	C11–Sn1–C12	164.0(7)
Sn2–O1	236.1(8)	C21–Sn2–C22	168.5(6)
		C31–Sn3–C32	172.1(10)
O1···N3	278.3(14)		
O1···N5	290.7(14)	Sn1···O2···N3	113.5(4)
O2···N3	286.1(14)	Sn1···O2···N5	116.4(4)
O2···N5	285.5(14)	Sn2···O1···N3	115.3(4)
		Sn2···O1···N5	113.3(4)
		N3···O1···N5	98.3(4)
		N5···O2···N3	97.8(4)

[a] Dotted lines refer to O–H···N hydrogen bonds.

hydrophilic because of a considerable crowding of H_2O ligands.

The supramolecular architecture of **1** in total is depicted in Fig. 2. All of the ribbons are arranged parallel to each other extending exclusively along the *c* axis, in that between two equivalent staples of ribbons in alternate positions (i.e. staples A and B) each of the terminal cyanide ligands seems to be involved in two O–H···NC bridges. Eight distinct O–H···N hydrogen bonds are thus active per formula unit. The resulting 3D framework of **1** is comparatively compact, although along *c* infinite, straight channels of a quasi-rectangular cross section (ca. 0.6×0.6 nm) extend, which accommodate the two strongly disordered H_2O molecules.

The Sn–N and Sn–O distances of **1** (Table 2) compare well with those found in earlier described coordination polymers containing Me_3Sn building blocks [10]. The C–N–Sn angles adopt throughout values close to 180°, while the C(Me)–Sn–C(Me) angles of the virtually *trans*-oriented methyl ligands deviate significantly from 180°. Even the various C–Co–C and Co–C–N angles of the $\{Co(CN)_6\}$ unit (not listed in Table 2) reflect notable deviations from the ideal octahedral values. The C(Me)–Sn distances vary between 206 and 218 pm, being on average slightly shorter than C(Me)–Sn distances in Me_3Sn building blocks.

The O···N distances of the O–H···NC hydrogen bonds of **1** are only slightly longer than those reported recently for an exemplary Me_3Sn-containing assembly [10]. The Sn–O–N angles listed in Table 2 deviate only weakly from 109° stating that the O–H···N fragments should be almost collinear. 'Unconventional' C–H···N hydrogen involving the tin-bonded methyl groups can be ruled out, as all C···N distances are longer than 375 pm.

4. IR/Raman-spectroscopic and XRD-properties of 1, 2 and 5

The frequencies of some characteristic infrared (IR) and Raman (Ra) active vibrations of **1**, **2** (prepared according to the two different routes) and **5** are listed in Table 3. It is difficult to deduce from the ν(CN) band positions that **1** contains also terminal cyanide ligands. For **2**, the appearance of five ν(CN) bands in total, without any pairwise (IR/Ra)-coincidence, would suggest the presence of $\{Co(CN)_6\}$ fragments of local D_{4h} symmetry. Although at least two Me_2Sn fragments of **1** have notably different environments, no more than three bands (IR + Ra) can be assigned to ν(SnC) vibrations. In contrast, **2** displays two intense $\nu(SnC)_s$ bands. It is also noted that the spectra of **2** depend slightly on the mode of the preparation. In the case of **5**, the comparatively larger number of Raman active ν(CN) bands is surprising. Interestingly, the host/guest system $[(n\text{Bu}_4\text{N})_{0.5}(Me_3Sn)_{3.5}Fe(CN)_6\cdot H_2O]$ [11] was found to behave similarly in displaying between 2026 and 3130 cm^{-1} even six Ra-active bands (and only four IR active

Table 3
Selected infrared and Raman bands (ν in cm^{-1}) of **1**, **2** and **5**

Vibration	**1**		**2** [a]		**2** [b]		**5**	
	IR	Ra	IR	Ra	IR	Ra	IR	Ra
ν(CN)	2154	2159	2150	2181	2151	2172	2044	2067
		2172	2166	2201	2166	2184	2065	2092
	2181			2206		2201		2111
	2196	2190						2136
								2146
ν_{as}(SnC) [c]	588	532	591		592		598	
		594 [e]						
ν_{s}(SnC) [c]		532		529 sh		528 sh		
		594 [e]						
ν_{as}(SnC) [d]	–	–	551	521	551	521	550	521
			558	551 [e]	558	551 [e]		553[e]
ν(CoC) [d]	448	477 [e]	442	472 [e]	440	474 [e]		
		492 [e]		483 [e]		482 [e]		

[a] Prepared by co-precipitation.
[b] Prepared according to Eq. (3) ($Sn:Br_2 = 1:2$).
[c] From Me_2Sn group.
[d] From Me_3Sn group.
[e] Very low intensity.

absorptions). An IR band at 598 cm^{-1} indicates the presence of Me_2Sn units.

The experimental powder X-ray diffractogram (XRD) of **2** (Fig. 4) differs notably from that of **1** (Fig. 3), suggesting the presence of a new solid phase and not of a mixture of **1** and **3**. This view is further supported by comparison with the reported [5] XRD of **3**. The XRD of **5** is dominated by one broad reflection centered at $2\Theta = 12°$ aside of a few sharp, but comparatively weak lines, suggesting essentially an amorphous nature.

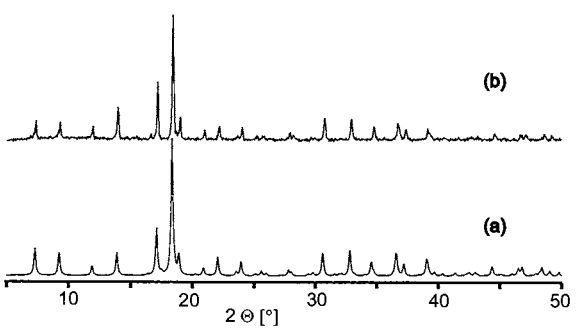

Fig. 3. XRDs of **1**: (a) simulated, (b) experimental diffractogram.

5. Solid-state NMR spectra of 1, 2 and 5

As the experimental XRD of bulk **1** agrees very satisfactorily with the XRD simulated from data of the single-crystal X-ray study (Fig. 3), it seems legitimate to discuss the results of a multinuclear (i.e. ^{13}C, ^{15}N, ^{59}Co, ^{119}Sn) CPMAS solid-state magnetic resonance study of **1** in terms of the asymmetric unit known from the crystallographic structure analysis. While the latter involves six nonequivalent methyl carbon and six cyanide nitrogen atoms, no more than two ^{13}C resonances (Fig. 5(a)) are found in the relevant chemical shift range (Table 4). The relative intensity of the two methyl ^{13}C signals is 1:2 within experimental error, so we assign the signal at $\delta_C = 17.8$ ppm to the methyl groups bonded to Sn3 and that at $\delta_C = 13.4$ ppm to those attached to Sn1 and Sn2. The ^{15}N spectrum was hard to attain since even an accumulation of 67 700 free induction decays

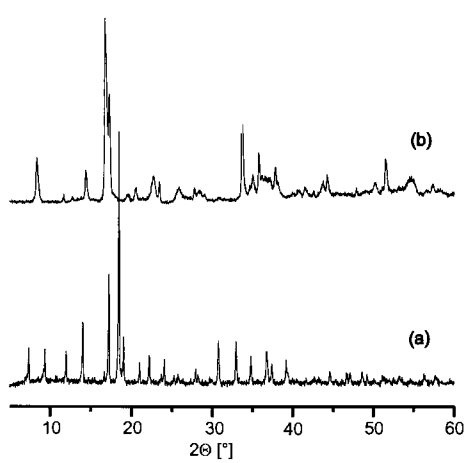

Fig. 4. Experimental XRDs of **1** (a) and **2** (b). **2** was prepared by co-precipitation.

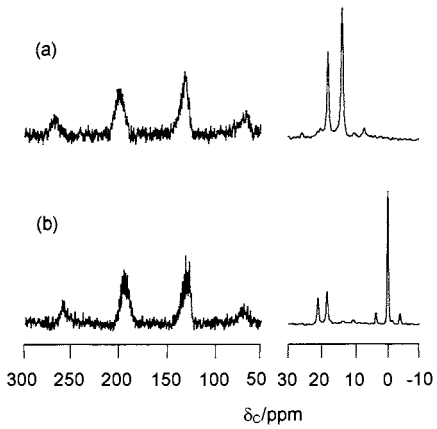

Fig. 5. Carbon-13 CPMAS spectra at 75.43 MHz and ambient probe temperature of (a) **1**, and (b) **2**. On the left is the ^{13}CN region and on the right (on a different frequency scale) the CH_2 and CH_3 regions. Spectrometer operating conditions: contact time 5 ms (a) and 20 ms (b); recycle delay 1.0 s; number of transients 1000 (a) and 600 (b); spin rate 4940 Hz (a) and 4660 Hz (b).

over a period of nearly 50 h gave only a modest S/N of ca. 4. However, two centerband signals of equal intensity are seen at $\delta_N = -132.3$ and -124.9 ppm. There is some indication of a third, weaker, peak at $\delta_N = -96.7$ ppm, but of this we cannot be certain. Such a situation would be consistent with terminal nitrogen resonances being to higher frequency than those of tin-coordinated nitrogens, although it would be expected [10] that O–H···NC hydrogen bonding would displace the latter again towards lower frequencies. Owing to the effect of site inequivalences and of coupling to the quadrupolar ^{59}Co and ^{14}N nuclei, just one very broad cyanide carbon resonance occurs, though with substantial partially-resolved fine structure. Instead of three (asymmetric unit), no more than two

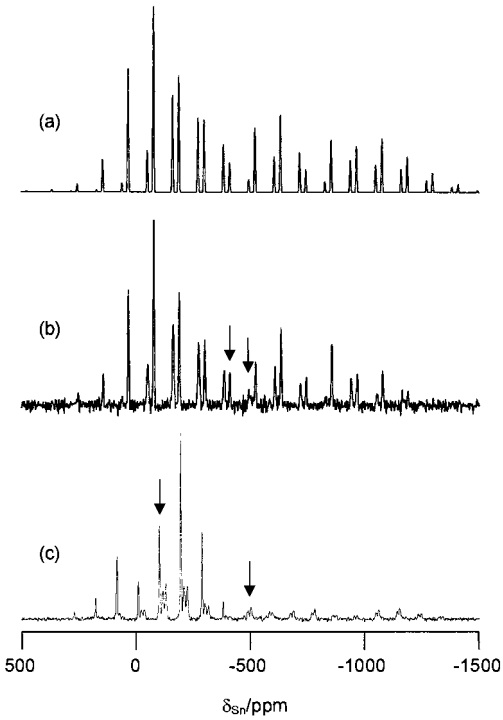

Fig. 6. Tin-119 CPMAS spectra at 111.79 MHz of (a) **1**, simulated (see text for parameters), (b) **1**, experimental, and (c) **2**, experimental. Spectrometer operating conditions: contact time 5 ms (b) and 20 ms (c); recycle delay 1.0 s (b) and 0.5 s (c); number of transients 55 000 (b) and 108 224 (c); spin rate 12.0 kHz (b) and 10.1 kHz (c). It is likely that the relatively high-speed spinning causes the sample temperature to rise significantly above ambient.

^{119}Sn centerbands (Fig. 6) appear as singlets (with an intensity ratio of 2:1 within experimental error) at rather low frequency, although still within the chemical shift range characteristic of hexa-coordinate tin [12]. One potential explanation of the constantly lower num-

Table 4
Chemical shifts (in ppm) of solid **1**, **2** and **5** [a]

Sample	$\delta(^{13}C)$ [b]	$^1J(^{119}Sn, ^{13}C)$ [b,c]	$\delta(^{13}C)$ [d]	$\delta(^{15}N)$	$\delta(^{119}Sn)$
1	13.4	1005	ca. 130	−132.4	−494
	17.8	1190		−124.8	−410
2	−0.4	555	ca. 130	−124.7 [f]	−102
	−1.95 [e]	n.o.		−121.4 [f]	
	18.2	1212		−122.4 [g]	−488
	21.0	1166		−118.8 [g]	−502
5	−1.7	635	ca. 170	ca. −121	−31 [h]
	22.7	n.o.			−139 [h]
	27.9	n.o.			

[a] All centerbands are singlets.
[b] From CH_3 groups.
[c] In Hz, determined from weak accompanying doublet.
[d] From the CN groups.
[e] Weak-absent in samples obtained by bromination of **3**.
[f] $|^1J(^{119}Sn, ^{15}N)| = 304$ and 292 Hz for the lines at $\delta_N = -124.7$ and -121.4 ppm, respectively.
[g] Minor peaks, possibly from an impurity.
[h] There is also a signal, with indeterminate centerband, in the Me_2Sn region.

ber of actually observed resonance lines than of those predicted from the asymmetric unit could be the assumption of a rapid (on the NMR timescale) periodic equilibration of the $\{Sn1(N1C1)_2\}$ and $\{Sn2(N2C2)_2\}$ fragments (see Fig. 1). The then surviving ^{119}Sn resonances (Table 4) would only distinguish between Sn3 and Sn1/Sn2. The less intense of the two methyl ^{13}C lines has the higher $J(^{119}Sn, ^{13}C)$ value (determined from the detectable satellite doublet arising from the presence of ^{119}Sn nuclei). Interestingly, a tentative determination of the C(Me)–Sn–C(Me) angles of **1** from adopting Lockhart's [13] empirical correlation of the $^1J(^{119}Sn, ^{13}C)$ value with that angle (Eq. (4)) leads to the values of:

$$C(Me)-Sn-C(Me)angle = \frac{^1J(^{119}Sn,\ ^{13}C)+778}{10.7} \quad (4)$$

167° for the averaged angle at Sn1/2 and of 186° (presumably folding back to 174°) for the angle at Sn3. Comparison with the crystallographically obtained data (Table 2), i.e. 167° versus 166.2°, and 174° versus 172.1°, reveals a surprisingly good agreement. The spinning sideband manifolds of the ^{119}Sn spectrum have been analyzed (Fig. 6) to give data on the shielding tensors. For both peaks the shielding asymmetry is zero within experimental error. This is reasonable for Sn3 but unexpected for Sn1/2 since the latter have *cis* bonds to two oxygen atoms. For other *trans*-cyanide-bridged

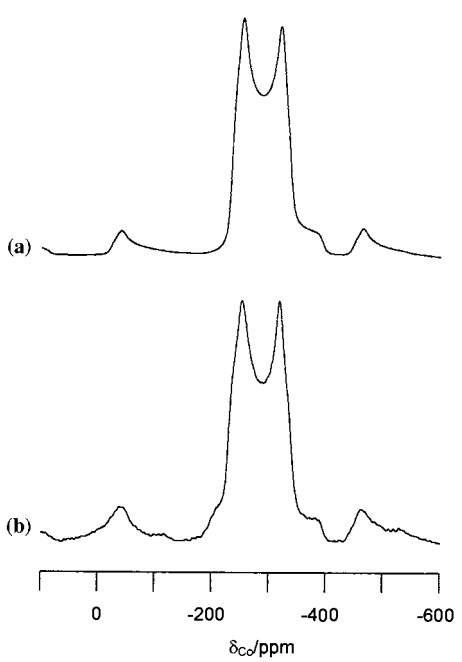

Fig. 7. Cobalt-59 direct polarization MAS spectra at 71.13 MHz of **1**: (a) simulated (see text for parameters), and (b) experimental. For the latter the spectrometer operating conditions are: pulse angle 22.5°; recycle delay 0.2 s; number of transients 20 000; spin rate 14.5 kHz. It is likely that the relatively high-speed spinning causes the sample temperature to rise significantly above ambient.

Me_3Sn systems, η has also been found [11,14] to be low (<0.3). The ^{119}Sn shielding anisotropies are $\zeta = 952$ and 865 ppm for the isotropic shifts $\delta_{Sn} = -410.6$ and -494.0 ppm, respectively. These values are significantly larger than those obtained for trigonal bipyramidal $SnMe_3$ groups for compounds **2** and **5** (see below) and related cyanide-bridged intermetallic systems [5b]. A single ^{59}Co-NMR band is found for **1** (Fig. 7(b)), with a typical powder bandshape arising from second-order quadrupolar effects. Spectral simulation (Fig. 7(a)) shows that $\delta_{iso}(^{59}Co) = -215$ ppm, the quadrupolar coupling constant is 11.6 MHz and the electric field gradient asymmetry parameter is 0.19.

The solid-state magnetic resonance spectra of co-precipitated **2** strongly suggest the absence of both **1** and **3**, as none of the main ^{13}C and ^{119}Sn resonances of these polymers were detected. The ^{119}Sn spectrum of **2** (Fig. 6(c)) displays one signal at a chemical shift ($\delta_{Sn} = -102$ ppm) typical of Me_3Sn, and a doublet ($\delta_{Sn} = -488$ and -502 ppm) at shifts typical of Me_2Sn, suggesting one *trans*-Me_3SnX_2 and two Me_2SnX_4 environments (with equal abundances) in the asymmetric unit. The Me_3Sn:Me_2Sn ratio is difficult to determine. The Me_2Sn signals show a wide spread of spinning sidebands typical of such groups, but an analysis is not feasible because of the low intensities of most sidebands. The structural conclusion is confirmed by the appearance (Fig. 5(b)) of two ^{13}C signals for the methyl groups of Me_2Sn but only one for Me in Me_3Sn. The intensity ratio of the three peaks is 1:1:3 (within experimental error) as expected and further confirmed by solution ^{1}H-NMR spectroscopy (see Section 7). Of course, in many Me_3Sn trigonal bipyramidal units of cyanide-bridged metal compounds rapid internal rotation about the N–Sn–N axis renders the three methyl groups equivalent.

The combined ^{119}Sn- and ^{13}C-NMR information makes it clear that the two methyl groups in a given Me_2Sn unit are also equivalent. The values of $|^1J_{SnC}|$, obtained from satellite peaks in the ^{13}C spectrum, show clearly that the C–Sn–C group in Me_2Sn must have *trans*-oriented (probably at approximately 180°) methyl groups. The cyanide ^{13}C signal of **2**, like that of **1**, consists of a complex band of partially-resolved lines from the effects of inequivalences and of a coupling to both ^{14}N and ^{59}Co. The ^{15}N spectrum of one sample of **2** contains two major lines, of equal intensity, and with ^{119}Sn satellites, plus two minor lines. A single, rather broad ^{59}Co signal is seen at $\delta_{Co} =$ ca. -260 ppm, with spinning sidebands spread over 6000 ppm, but discernable second-order structure.

The ^{13}C and solution ^{1}H spectra of **5** confirm the presence of both Me_2Sn and Me_3Sn entities, although the difficulty of locating satellite doublets arising from ^{119}Sn, ^{13}C coupling for the former does not allow any prediction of the C(Me)–Sn–C(Me) angles. The pair of

peaks assignable to Me_2Sn carbons is at rather high frequency ($\delta_C = 27.9$ and 22.7 ppm). In the ^{119}Sn spectrum, one centerband typical of *trans*-$Me_3Sn(NC)_2$ fragments appears ($\delta = -138$ ppm), while a peak at -30 ppm may be best assigned to either of the fragments: {*trans*-$Me_3Sn(NC)(OH_2)$} or {*trans*-$Me_3Sn(OH_2)_2$} [10]. The centerband ^{119}Sn resonance of octahedrally supplemented Me_3Sn fragments is not clearly detectable, although several weak lines form a spinning sideband manifold within the expected range. Interestingly, the two quite characteristic ^{119}Sn centerbands of $[(Me_3Sn)_4Fe(CN)_6]$ (**6**) [8] at -108 and $+47$ ppm seem to appear as well, and gain in intensity during the course of the NMR experiment. Uptake of thermal energy owing to extended, rapid spinning might be responsible for a more efficient separation of the two 'non-alloyed' products **6** and $[(Me_2Sn)_2Fe(CN)_6 \cdot x H_2O]$. Only a poor-quality ^{15}N spectrum of **5** could be obtained. This showed a broad signal at $\delta_N \sim -121$ ppm, with possible (but ill-defined) fine structure.

6. Conclusions

In aqueous solution, Me_2Sn^{2+} and $[Co(CN)_6]^{3-}$ ions assemble spontaneously to the novel coordination polymer $[(Me_2Sn)_3\{Co(CN)_6\}_2 \cdot 6H_2O]$ (**1**) wherein, according to the more structure-related formulation: $[(Me_2Sn)(Me_2Sn \cdot 2H_2O)_2\{Co(CN)_6\}_2 \cdot 2H_2O]$, only one of the three Me_2Sn units reaches hexacoordination exclusively via $CN \rightarrow Sn$ bonding. The partial coordination of water molecules to tin atoms leads to infinite, planar ribbons carrying at their edges all Sn-coordinated H_2O molecules, which helps in achieving a three-dimensional supramolecular architecture by extensive O–H···NC hydrogen bonding. A structurally related coordination polymer containing also Me_2Sn units is $[(Me_2Sn)_3(PO_4)_2 \cdot 8H_2O]$ [15], wherein infinite, ribbon-like building blocks carry similarly H_2O molecules at their edges, although here the ribbon profiles are oriented alternately horizontal and vertical. Another potential homologue of **1** is the coordination polymer $[(Pr_2Sn)_3\{Fe(CN)_6\}_2 \cdot 4H_2O]$ (Pr = propyl) the crystal structure of which is, however, still unknown [16].

While **1** in its hydrated form seems to be energetically more favorable than an anhydrous framework, wherein all coordination sites of the $\{Me_2Sn\}$ units would be occupied by cyanide N atoms (12:12), a more Prussian-blue-like 3D framework may readily be envisioned for anhydrous **2**. Thus, planar layers resulting formally from desolvated ribbons of **1** after infinite expansion along *b* (Fig. 1) might be regularly stacked and connected via $\{Me_3Sn\}$ units by means of the still terminal cyanide ligands oriented perpendicular to the planes. The new framework would possess along the (original) *c* axis infinite, linear channels of approximately rectangular cross sections (ca. 0.8×1.1 nm). It is, on the other hand, true that too voluminous frameworks are usually circumvented by the formation of more compact architectures (e.g. by mutually interpenetrating frameworks [17]).

Although the crystal structure of 1 differs notably from that of $Zn_3\{Co(CN)_6\}_2 \cdot x H_2O$ [18] and the structures of related members of the Prussian blue family [19], both **1** and **2** are likely to also display catalytic properties. Like the non-organometallic double metal cyanides, these coordination polymers dissociate partially into their Lewis basic and Lewis acidic components. For instance, **2** and **5** are, like **1**, completely soluble in D_2O–NaOD (pH: ca. 8–9), and these solution give rise to two distinct ^1H-NMR signals of the hydrated Me_2Sn^+ and Me_3Sn^+ ions the intensity ratio of which helps determining independently the Me_2Sn–Me_3Sn ratio of the sample in question.

The selective bromination of **3** affording quite unexpectedly **2**, opens a new perspective for the bromination of other organotin metal cyanide systems.

It seems to be more difficult ascribing a reasonable structure to **5**. Although the XRD of the practically amorphous, faintly greenish precipitate does not display any of the stronger reflections of **6**, ^{119}Sn resonances clearly indicative of this species emerge in the solid-state spectrum of **5** (vide supra). Another unexpected feature is that **5** turns blue after more rigorous drying (e.g. in vacuo). In D_2O–NaOD solution, the blue species gives rise to a significantly larger Me_3Sn–Me_2Sn ratio than 3:1 (as expected for **5**). Obviously, more detailed information is required to clarify the nature of **5**.

7. Experimental

7.1. Methods and instrumentation

All operations could be carried out without special protection from atmosphere. IR spectra were obtained on a Perkin–Elmer IR 1720 instrument, and Raman spectra on a Ramanow U-1000 spectrometer of Jobin Yvon. X-ray powder diffractograms (XRD) were taken on a Phillips X'PERT diffractometer ($Cu–K_\alpha$) equipped with a Ni filter, and solution ^1H-NMR spectra either on a Bruker AM 360 or a Varian Gemini 200 spectrometer.

Solid-state NMR: the solid-state NMR spectra were recorded on a Varian VXR 300 spectrometer operating at frequencies of 75.4, 11.9, 30.4 and 71.1 MHz for ^{13}C, ^{119}Sn, ^{15}N and ^{59}Co, respectively. Crosspolarization with high-powder proton decoupling was used for all spectra except ^{59}Co where direct polarization was used. The ^{113}C and ^{15}N spectra were recorded with a Doty

Scientific probe with 7 mm o.d. rotors, but for the ^{119}Sn and ^{59}Co spectra a faster-spinning Doty Scientific probe with 5 mm o.d. rotors was used. Acquisition conditions are given in the figure captions. Chemical shifts are reported, with the high-frequency positive convention, in ppm relative to the signals for $SiMe_4$, $SnMe_4$, NH_4NO_3 (nitrate line), and $K_3[Co(CN)_6]$(aq.) for ^{13}C, ^{119}Sn, ^{15}N, and ^{59}Co, respectively. Shielding tensor components are defined by $|\sigma_{ZZ}-\sigma_{iso}| \geq |\sigma_{XX}-\sigma_{iso}| \geq |\sigma_{YY}-\sigma_{iso}|$, with anisotropy $\zeta = \sigma_{ZZ}-\sigma_{iso}$ and $\eta = (\sigma_{YY}-\sigma_{XX})/\zeta$. Analysis of spinning sideband manifolds was carried out using either an in-house computer program [20] or the STARS Varian software. Analysis of the ^{59}Co bandshape for quadrupolar effects used the STARS software. The 90° pulse for the ^{59}Co direct polarization spectra was calibrated using an aqueous solution of $K_3[Co(CN)_6]$.

The single-crystal X-ray study of **1** was carried out on a Hilger & Watts Y290 four-circle diffractometer equipped with a low-temperature device (Table 1). Positions of heavy atoms were determined by direct methods, and the positions of the lighter C-, N- and O-atoms by means of difference Fourier and least-squares calculations. All non-hydrogen atoms except N1, N6, C1, C5, C6, C22, C31 and C32 were refined anisotropically. The latter atoms could be refined isotropically. H atoms could not be localized and were also refined isotropically in keeping a fixed C–H distance of 96.0 pm.

7.2. Preparation of *1*, *2* and *5*

$[(Me_2Sn)_3\{Co(CN)_6\}_2 \cdot xH_2O]$ (**1**): a clear solution of Me_2SnCl_2 (3.30 g, 0.015 mol) in 50 ml of H_2O was added slowly to a solution of $K_3[Co(CN)_6]$ (3.32 g, 0.01 mol) in 50 ml of H_2O. The white voluminous precipitate which appears after up to 1 min is separated from the filtrate, washed subsequently with H_2O and Et_2O and dried finally in vacuo (oil pump). Yield: 7.6 g (83%), decomposition temperatures: 200/360°C (green/black). Elemental analysis $C_{18}H_{22}N_{12}O_2Co_2Sn_3$ ($x = 2$): Anal. Calc. C, 23.59; H, 2.42; N, 18.35; Co, 12.87; Sn, 39.28. Found: C, 23.65; H, 2.23; N, 17.65; Co, 12.87; Sn, 38.42%.

$[(Me_2Sn)(Me_3Sn)Co(CN)_6]$ (**2**; co-precipitation): a solution of Me_2SnCl_2 (2.19 g, 0.01 mol) and Me_3SnCl (2.0 g, 0.01 mol) in 50 ml of H_2O were added under vigorous stirring to a solution of $K_3[Co(CN)_6]$ (3.32 g, 0.01 mol) in 50 ml of H_2O. After filtration of the spontaneously formed white precipitate, subsequent washing with H_2O and Et_2O and drying in vacuo (oil pump), 4.8 g of analytically pure **2** (yield: 91%) are obtained. Thermal decomposition 300°C (blue). Elemental analysis $C_{11}H_{15}N_6CoSn_2$: Anal. Calc. C, 25.04; H, 2.87; N, 15.93; Co, 11.17; Sn, 45.00. Found: C, 25.03; H, 2.92; N, 15.48; Co, 11.60; O, 0.50; Sn, 43.53%. The solution ^{1}H-NMR spectrum of **2** (solvent: D_2O–NaOD, pH ca. 9) confirms independently a Me_3Sn–Me_2Sn ratio of 1:1.

2 (by bromination of **3**): a solution of Br_2 (either 0.22 ml = 4.2 mmol or 0.01 ml = 0.2 mmol) in 10 ml of methanol was added slowly and in the dark to a suspension of $[(Me_3Sn)_3Co(CN)_6]$ (**3**) (either 1.0 g = 1.4 mmol or 0.9 g = 1.27 mmol), kept in a three-necked flask equipped with a cooler and a dropping funnel. After stirring over ca. 12 h, the mixture is briefly heated up to the boiling point. After filtration, washing of the residue with MeOH and Et_2O and drying in vacuo, white powders of **2** are obtained in quantitative yields. Elemental analysis $C_{11}H_{15}N_6CoSn_2$: Anal Calc. C, 25.04; H, 2.87; N, 15.93; Co, 11.17; Sn, 45.00. Found: 24.61/24.70; H, 2.81/2.86; N, 16.00/15.62; Co, 11.28/11.30; Sn, 45.39/45.36%.

Preparation of **5**: a solution of Me_2SnCl_2 (2.19 g, 0.01 mol) and Me_3SnCl (4.0 g, 0.02 mol) in 50 ml of H_2O was added under stirring to a solution of $K_4[Fe(CN)_6]$ (4.22 g, 0.01 mol) in 50 ml of H_2O. The almost white, paste-like solid obtained after filtration and washing (H_2O, Et_2O) is transformed after drying (avoiding vacuum) into a faintly greenish powder that turns black at 350°C. Final yield: 7.1 g (95%). Elemental analysis $C_{14}H_{30}N_6O_3FeSn_3$ ($x = 3$): Anal. Calc. C, 22.65; H, 4.07; N, 11.32; Fe, 7.52; O, 6.47; Sn, 47.97. Found: C, 21.31; H, 7.76; N, 11.51; Fe, 7.93; O, 7.85; Sn, 43.25%.

Note added in proof: briefly after the submission of our manuscript, crystal structures of the anhydrous 'homologues' of **1**, $[(R_2Sn)_3\{Co(CN)_6\}_2]$ with R = vinyl, *n*-propyl and *n*-butyl, have been reported [22]. In these coordination polymers, all four coordination sites of each $\{R_2Sn\}^{2+}$ unit are in fact occupied by cyanide N atoms (cf. Section 6).

8. Supplementary material

Full details of the crystal structure determination of **1** have been deposited with the Cambridge Crystallographic Data Centre, CSD 407641 [21]. Copies of the data can be obtained free of charge from the Director, CCDC, 12 Union Road, Cambridge CB2 1EZ, UK (Fax: +44-1223-336033; e-mail: deposit@ccdc.cam.ac.uk or www: http://www.ccdc.cam.ac.uk).

Acknowledgements

This work was supported by the Deutsche Forschungsgemeinschaft, DFG (Schwerpunktprogramm: Nanoporöse Wirt/Gast-Systeme) and the Fonds der Chemischen Industrie. The authors are

grateful to S. Samba for valuable technical assistance. The extensive CPMAS NMR work was supported by the UK EPSRC (through the National Solid-State NMR Service based at Durham).

References

[1] R.A. Livigni, R.J. Herold, O.C. Elmer, S.L. Aggarwal, ACS, Symp. Ser. No. 6 (polyethers) Washington, DC, 1975, p. 20.
[2] J.L. Schuchardt, S.D. Harper, Proceedings of the 32nd Annual Polyurethane Technical/Marketing Conference (Oct. 14, 1989) p. 360.
[3] J. Hofmann, Patent WO 99/19063 (22.04.99). For a more detailed survey of the development taking place in this field, the IPC Group C 08 G65/10 should be consulted.
[4] (a) Polymeric $Me_2Sn(CN)_2$: J. Konnert, D. Britton, Y.M. Chow, Acta Crystallogr. Sect. B 28 (1972) 180. (b) Polymeric $Me_2Sn\{N(CN)_2\}_2$: Y.M. Chow, Inorg. Chem. 10 (1971) 1938.
[5] (a) K. Yünlü, N. Höck, R.D. Fischer, Angew. Chem. 97 (1985) 863; Angew. Chem. Int. Ed. Engl. 24 (1985) 879. (b) U. Behrens, A.K. Brimah, T.M. Soliman, R.D. Fischer, D.C. Apperley, N.A. Davies, R.K. Harris, Organometallics 11 (1992) 1718.
[6] Y. Sasaki, H. Imoto, O. Nagano, Bull. Chem. Soc. Jpn. 57 (1984) 1417.
[7] See: S. Boué, M. Gielen, J. Nasielski, J.-P. Lieutnant, R. Spielmann, Bull. Soc. Chim. Belg. 78 (1969) 135.
[8] S. Eller, P. Schwarz, A.K. Brimah, R.D. Fischer, D.C. Apperley, N.A. Davies, R.K. Harris, Organometallics 12 (1993) 3232.
[9] M. Heibel, G. Kumar, C. Wyse, P. Bukovec, A.B. Bocarsly, Chem. Mater. 8 (1996) 1504.
[10] P. Schwarz, E. Siebel, R.D. Fischer, N.A. Davies, D.C. Apperley, R.K. Harris, Chem. Eur. J. 4 (1998) 919.
[11] P. Schwarz, S. Eller, E. Siebel, T.M. Soliman, R.D. Fischer, D.C. Apperley, N.A. Davies, R.K. Harris, Angew. Chem. 108 (1996) 1611; Angew. Chem. Int. Ed. Engl. 35 (1996) 1525.
[12] Actually, relatively few quasi-octahedral R_2Sn-derivatives with $\delta(^{119}Sn)$ values around -400 ppm have been reported, e.g. (a) W.F. Howard Jr., R.W. Crecely, W.H. Nelson, Inorg. Chem. 24 (1985) 2204. (b) A. Lycka, J. Holecek, B. Schneider, J. Straka, J. Organomet. Chem. 389 (1990) 29.
[13] (a) T.P. Lockhart, W.F. Manders, J. Am. Chem. Soc. 109 (1987) 7015. (b) T.P. Lockhart, F. Davidson, Organometallics 6 (1987) 2478.
[14] R.K. Harris, D.C. Apperley, N.A. Davies, R.D. Fischer, Bull. Magn. Reson. 15 (1993) 22.
[15] J.P. Ashmore, T. Chivers, K.A. Kerr, J.H.G. van Roode, Inorg. Chem. 16 (1977) 191.
[16] A. Bonardi, C. Carini, C. Pelizzi, G. Pelizzi, G. Predieri, P. Tarasconi, M.A. Zoroddu, K.C. Molloy, J. Organomet. Chem. 401 (1991) 283.
[17] S.R. Batten, R. Robson, Angew. Chem. 110 (1998) 1558; Angew. Chem. Int. Ed. Engl. 37 (1998) 1460.
[18] D.F. Mullica, W.O. Milligan, G.W. Beall, W.L. Reeves, Acta Crystallogr. Sect. B 34 (1978) 3558.
[19] G. Malecki, A. Ratuszna, Powder Diffraction 14 (1999) 25.
[20] J. Ascenso, H. Bai, R.K. Harris, L.H. Merwin, Sideband fitting program, University of Durham, 1985, 1987, 1991.
[21] For a recent discussion in the Internet on the justification of empirical absorption corrections (like DIFABS), see: http://crystsun1.unige.ch/stxnews/stx/discuss/dis-dif2.htm.
[22] T. Niu, A.J. Jacobson, Inorg. Chem. 38 (1999) 5346.